

General Disclaimer

One or more of the Following Statements may affect this Document

- This document has been reproduced from the best copy furnished by the organizational source. It is being released in the interest of making available as much information as possible.
- This document may contain data, which exceeds the sheet parameters. It was furnished in this condition by the organizational source and is the best copy available.
- This document may contain tone-on-tone or color graphs, charts and/or pictures, which have been reproduced in black and white.
- This document is paginated as submitted by the original source.
- Portions of this document are not fully legible due to the historical nature of some of the material. However, it is the best reproduction available from the original submission.

NASA Technical Memorandum 83346

(NASA-TM-83346) DESIGN ANALYSIS OF A
SELF-ACTING SPIRAL-GROOVE RING SEAL FOR
COUNTER-ROTATING SHAFTS (NASA) 12 P
HC 402/HF A01

N83-23306

CSCL 21E

G3/07 Unclas
03474

Design Analysis of a Self-Acting Spiral-Groove Ring Seal For Counter-Rotating Shafts

Eliseo DiRusso
Lewis Research Center
Cleveland, Ohio



Prepared for the
Nineteenth Joint Propulsion Conference and Technical Display
cosponsored by the AIAA, SAE, and ASME
Seattle, Washington, June 27-29, 1983

NASA

DESIGN ANALYSIS OF A SELF-ACTING SPIRAL-GROOVE
RING SEAL FOR COUNTER-ROTATING SHAFTS

ORIGINAL PAGE IS
OF POOR QUALITY

Eliseo DiRusso
National Aeronautics and Space Administration
Lewis Research Center
Cleveland, Ohio 44135

Summary

A spiral groove ring seal of a nominal 16.33 cm (6.43 in.) diameter for sealing fan bleed air between counter-rotating shafts in advanced turbofan engines was analyzed. The analysis focused on the lift force characteristics of the pressure balanced spiral grooves. A computer program¹ for predicting the performance of gas lubricated (compressible fluid) spiral groove face seals was employed in the analysis. The computer program was used to optimize the spiral groove geometry to produce maximum lift force for steady state conditions. Load capacity curves (lift force as function of film thickness) were calculated for advanced turbofan engine typical operating conditions at relative seal speeds ranging from 17 850 to 29 800 rpm, sealed air pressures from 6 N/cm² (9 psi) absolute and temperatures from 95° to 327° C (203° to 620° F). The relative seal sliding speed range was 152 to 255 m/sec (500 to 836 ft/sec). The load carrying capacity of the spiral grooves was calculated for various groove depths, spiral groove angles, groove to land width ratios and film thicknesses. Three geometric parameters of the spiral grooves were optimized to produce maximum lift force; these were, groove depth, spiral groove angle and groove to land width ratio. The optimum values for these parameters were found to be:

Groove depth - 0.0178 mm (0.0007 in.)*
Spiral groove angle - 20°
Groove to land width ratio - 2.50

The analysis revealed that, for steady state conditions, the spiral groove geometry can be optimized to produce sufficient lift force to maintain a minimum film thickness of approximately 0.0037 mm (0.00015 in.) and an average film thickness of approximately 0.0047 mm (0.00019 in.) over the entire operating range of typical advanced turbofan engines. The spiral groove seal has potential to operate at the high sliding speeds (255 m/sec (836 ft/sec)) of this application without distress due to friction because the seal faces are separated by a thin air film of relatively high film stiffness.

Introduction

A self-acting spiral groove inter-shaft ring seal of nominal 16.33 cm (6.43 in.) diameter for sealing fan bleed air between counter-rotating shafts in advanced turbofan engines was analyzed. The analysis focused on the lift force characteristics of the spiral grooves. The spiral groove inter-shaft ring seal shown in figure 1 is a new seal concept which has potential application in sealing fan bleed air between two counter-rotating shafts in advanced turbofan aircraft engines. This is a difficult sealing application for any

contacting type seal because the counter-rotating shafts set up very high sliding speeds for the seal which are on the order of 255 m/sec (836 ft/sec). In addition to the high sliding speed, the seal must accommodate approximately 0.64 cm (0.25 in.) of axial translation due to relative axial motion between the two shafts.

The inter-shaft ring seal application is an excellent example of the need for applying self-acting gas lubricated bearing technology to contacting type seals. Application of a self-acting geometry in the form of spiral grooves to the faces of the ring seal housing (fig. 1) will maintain a thin air film of relatively high stiffness between the seal ring and the housing thereby enabling the seal to operate in a non-contacting mode over the entire engine operating range. The seal could then potentially operate at 255 m/sec (836 ft/sec) sliding speed and accommodate axial translations of 0.64 cm (0.25 in.) and have leakage rates consistent with contacting type seals.

When spiral grooves are employed in a seal as a film generating mechanism, the following are generally required in order to calculate the axial force equilibrium:

- (1) Film load capacity curve (lift force as function of film thickness)
- (2) Minimum film thickness over the operating range
- (3) Optimization of the spiral groove geometry to maximize the lift force for a given seal envelope size and operating condition

The objective of this paper is to determine the feasibility of using spiral grooves in the inter-shaft seal and to calculate the load capacity curves, calculate minimum film thickness (for steady state) over a typical turbofan engine operating range and to optimize the spiral groove geometry to produce maximum lift force for a given seal envelope size. A NASA-Lewis developed computer program¹ was employed to analytically achieve these objectives.

Discussion and Analysis

Seal Operating Features

Figure 1 shows the inter-shaft seal concept chosen for this study. The housing which contains the carbon ring rotates with the inner shaft. The carbon ring is bounded on its outside diameter by the outer shaft which counter-rotates with respect to the inner shaft. As the shafts rotate, the carbon ring expands into the outer shaft and assumes the speed of the outer shaft. The relative sliding speed between the carbon ring and the inner shaft can approach 255 m/sec (836 ft/sec). It should be noted that the carbon ring may require a radial split line to limit hoop stresses due to rotation and to assure that the carbon ring will rotate with the outer shaft. Relative axial translations between the inner and outer shafts of up to 0.64 cm (0.25 in.) due to thermal expansion are possible over the design operating range. This translation causes the carbon ring to ap-

*This value of groove depth is optimum for a film thickness of 0.0051 mm (0.0002 in.).

proach one of the two housing faces. The spiral grooves on the housing faces generate a very high lift force as the carbon ring approaches either face thereby maintaining a fluid film between the carbon ring and the housing face.

Figure 2 is a schematic drawing of the seal showing it in a neutral position (equal clearance on either side of the carbon). The total axial clearance between the carbon ring and the housing face is 0.0203 mm (0.0008 in.) or 0.0102 mm (0.0004 in.) per side when the seal is centered in the housing. The air flow through the seal is shown in figure 2. P_1 is the high pressure and the pressure drop from P_1 to P_2 occurs across the seal dam. The porting shown in figure 2 is designed such that the spiral grooves are bounded by the sealed pressure (P_1) at both the outside and inside diameters, hence, there is no pressure difference across the spiral grooves. This is known as a pressure balanced spiral groove concept. The pressure balanced concept isolates the spiral groove flow from the seal leakage flow so that the spiral groove performance is not subject to any ill effects due to seal leakage flow.

Transients such as pressure and thermal expansion which occur over the engine operating range will change the axial force equilibrium of the seal thus causing the carbon seal ring to approach one of the housing faces as shown in figure 3. As the clearance between the carbon seal ring and one of the housing faces approaches zero clearance, the spiral grooves generate a very high lift force. The lift force increases exponentially with reduction in clearance until a clearance is achieved at which axial force equilibrium is restored. The forces which enter into the axial force equilibrium are pressure area forces on the carbon ring, friction force between the carbon ring and the outer shaft (produced by relative axial translations of the shafts) and the lift force generated by the spiral grooves.

Spiral Groove Analysis

As stated previously, the analysis was directed to predicting the spiral groove load capacity curves and to optimize the spiral groove geometry for steady state conditions. A NASA-Lewis developed computer program¹ was used in the analysis. The program predicts the performance of spiral groove gas lubricated (compressible fluid) face seals for either inward or outward pumping spiral groove configurations; the form of which are logarithmic spirals. An inward pumping spiral groove configuration pumps the fluid radially from the outer region of the seal towards the center; conversely, an outward pumping configuration pumps the fluid radially from the inner region of the seal towards the outside. Inputs to the program are spiral groove geometric data, misalignment angles, speed, fluid viscosity, temperatures and pressures. Outputs which were used were fluid film lift force, film thickness, and pressure distribution.

The film pressure profile is calculated by solving the governing fluid equation (Reynolds equation) using a converging finite difference approximation. The analytical treatment is based on the narrow groove theory² modified for logarithmic spiral groove geometry.

The seal ring and spiral groove geometry are shown in figure 4. The inside and outside diameters of the seal ring were set by the available space in a typical advanced turbofan engine. The spiral groove outside radius (r_o), and the seal

band radius (r_b) were arbitrarily selected to maximize the radial length of the spiral grooves ($r_o - r_b$) within the available radial space. Having specified the above parameters; the spiral groove depth, spiral groove angle and groove to land width ratio are left as the lift force optimizing parameters. The spiral groove optimization was carried out for engine operating condition 1 (see table 1).

Figure 5 is a plot of spiral groove depth for maximum lift force as a function of film thickness. Data for this plot were obtained by generating a family of curves of lift force as a function of groove depth. The groove depth associated with the maximum lift force for each film thickness was then taken from this family of curves and plotted against their respective film thicknesses. The plot shows that the maximum lift force occurs at a film thickness to groove depth ratio of approximately 0.29 for film thicknesses above approximately 0.0025 millimeter (0.0001 in.). Although this curve was plotted using the optimized conditions of this analysis, it applies generally for spiral groove seals.

The desired operating film thickness was set at 0.0051 mm (0.0002 in.), hence the groove depth according to figure 5 should be 0.0178 mm (0.0007 in.) for maximum lift force to occur at 0.0051 mm (0.0002 in.) film thickness. Computer runs were then made for a groove depth of 0.0178 mm (0.0007 in.) to determine the combination of spiral groove angle and groove to land width ratio at which the maximum lift force occurs. Figure 6 is a plot of lift force as a function of spiral groove angle (all other parameters were held constant). The plot shows the lift force peaking out at approximately 20°. Figure 7 is a plot of lift force as a function of groove to land width ratio (all other parameters were held constant). This plot shows the lift force peaking out at a groove to land width ratio of approximately 2.50. Figure 8 is a plot of lift force as a function of groove depth (all other parameters were held constant). This plot shows the lift force peaking out at a groove depth of approximately 0.0178 mm (0.0007 in.) as expected since this is the optimum groove depth for the 0.0051 mm (0.0002 in.) film thickness as discussed previously.

The computer program used in the analysis assumed an infinite number of spiral grooves. This assumption is justified when the number of grooves is 50 or more³ hence the previously calculated optimum parameters will be valid for any number of grooves over 50. The number of grooves must also comply with the assumptions of the narrow groove theory⁴ to be accurately modeled. The use of this theory is justified for groove aspect ratios (groove length to width ratio) greater than 5. Figure 9 shows the spiral grooves to scale for an 80 groove configuration. The groove aspect ratio for the 80 groove configuration is approximately 8 and is in agreement with the narrow groove assumption.

Figure 10 shows plots of lift force as a function of film thickness for operating condition 1. The dashed curve is for a constant film thickness to groove depth ratio of 0.29 and therefore shows the true optimum lift force for any given film thickness. The solid curve gives the actual performance (compromized optimum lift force) for the constant groove depth of 0.0178 mm (0.0007 in.). This groove depth produces optimum lift force only at the desired operating film thickness of 0.0051 mm (0.0002 in.), hence, it is labeled as

compromized optimum in figure 10. The curves illustrate the difference between the true optimum and the compromised optimum which results from the necessity of having to choose a unique groove depth for a specific design.

Figure 11 shows lift force as a function of film thickness for the four operating conditions shown in table I. The lift force optimization was performed for engine operating condition 1; hence the lift force curve for this condition is optimum. The curves for engine operating conditions 2, 3, and 4 were calculated for the spiral groove angle, groove to land width ratio and groove depth which were optimized for engine condition 1. Therefore, the curves for engine operating conditions 2, 3, and 4 are off-design and are not necessarily optimum.

The operating steady-state film thickness range for each of the four operating conditions can be determined by consulting the appropriate curve in figure 11. The anticipated range of axial frictional and pressure-area forces which must be counteracted by the spiral groove lift force are given in table II. Entering the curves of figure 11 with these respective values of lift force yields the operating film thickness ranges shown in table II. The table shows that the minimum steady-state film thickness found over the entire engine operating range was 0.0037 mm (0.00015 in.) and the average film thickness was 0.0047 mm (0.00019 in.).

Summary of Results

An analysis was performed for a self-acting spiral groove inter-shaft ring seal of 16.33-cm (6.43-in.) nominal diameter operating in air to determine the lift characteristics of the spiral groove geometry. A potential use for this type of seal is for sealing fan bleed air between counter-rotating turbofan engine shafts. A computer program for predicting the performance of gas lubricated spiral groove face seals was used in the analysis to determine the optimum spiral groove geometry for maximum lift force and to generate the load capacity curves (lift force as function of film thickness). The analysis was performed for four typical turbofan engine operating conditions at relative seal speeds ranging from 17 850 to 29 800 rpm, sealed air pressures from 6 to 42 N/cm² (9 to 60 psi) absolute and temperatures from 95° to 327° C (203° to 620° F). The relative seal sliding speed range was 152 to 255 m/sec (500 to 836 ft/sec). The load carrying capacity of the spiral grooves was calculated for various groove depths, spiral groove angles, groove to land width ratios and film thicknesses. The analysis was for a pressure balanced spiral groove system operating at the sealed pressure.

The analysis produced the following results:

1. The spiral groove geometry can be optimized to produce sufficient lift force such that the self acting ring seal will operate in a non-contacting mode for steady state conditions even with the space limitation of typical advanced turbofan engine inter-shaft seal applications.

2. The minimum steady-state film thickness over the entire anticipated advanced turbofan engine operating range was 0.0037 mm (0.00015 in.) and the average film thickness was approximately 0.0047 mm (0.00019 in.) which is satisfactory for this application.

3. The following optimum values of the spiral groove geometrical features were found to produce maximum lift force for engine operating condition 1 (see table I):

Groove depth - 0.0178 mm (0.0007 in.)*

Spiral groove angle - 20°

Groove to land width ratio - 2.50.

To reduce leakage, it is advantageous to use a low leakage contacting-type seal instead of a labyrinth for the inter-shaft seal in advanced turbofan engines. The inherently high sliding speed (255 m/sec (836 ft/sec)) of inter-shaft seals produces very high friction and wear in contacting type seals using conventional materials. The use of spiral grooves enables a contacting type seal to operate in a noncontacting mode thereby eliminating the friction and wear problems and permitting the use of conventional seal materials at these speeds.

References

1. Mechanical Engineering Laboratory of The Franklin Research Center, A Division of The Franklin Institute: Spiral Groove Face Seal Computer Program (SEALSG). Franklin Research Center Project Number 21464, March 1979.
2. Elrod, H. G.: A Generalized Narrow Groove Theory For The Gas Lubricated Herringbone Thrust Bearing. Proceedings of The Fourth Gas Bearing Symposium, vol. 2, Univ. of Southampton, England, April 1969, pp. 18-1 to 18-21.
3. Muijderland, E. A.: Spiral Groove Bearings. Philips Technical Library, Springer-Verlag, New York, 1966.

*This value of groove depth is optimum for a film thickness of 0.0051 mm (0.0002 in.).

TABLE I. - TYPICAL SEAL ENVIRONMENTAL CONDITIONS FOR VARIOUS ENGINE OPERATING CONDITIONS

Engine operating condition	Sealed air pressure, P ₁ absolute		Sealed air temperature, T ₁		Downstream air pressure, P ₂ absolute		Downstream air temperature, T ₂		Sealed air viscosity		Relative seal speed, ^a rpm
	N/cm ²	psi	°C	°F	N/cm ²	psi	°C	°F	N·sec/cm ²	lbf·sec/in. ²	
1	41.4	60.0	327	620	11.0	16.0	149	300	0.302x10 ⁻⁸	0.438x10 ⁻⁸	29 800
2	11.6	16.8	95	203	10.3	15.0	110	230	.215x10 ⁻⁸	.312x10 ⁻⁸	17 850
3	6.2	9.0	115	239	2.7	3.9	116	240	.224x10 ⁻⁸	.325x10 ⁻⁸	23 400
4	17.2	25.0	298	569	1.2	1.7	132	270	.292x10 ⁻⁸	.424x10 ⁻⁸	28 050

^aThe relative seal speed is the sum of the absolute speeds of the inner and outer shafts.

TABLE II. - OPERATING FILM THICKNESS RANGES

Engine operating condition	Anticipated range of axial force which must be counteracted by spiral groove lift force		Operating film thickness range (from fig. 11)	
			mm	in.
	N	lb		
1	445 to 890	100 to 200	0.0037 to 0.0056	0.00015 to 0.00022
2	178 to 311	40 to 70	.0042 to .0057	.00017 to .00022
3	222 to 445	50 to 100	.0038 to .0056	.00015 to .00022
4	400 to 756	90 to 170	.0038 to .0054	.00015 to .00021

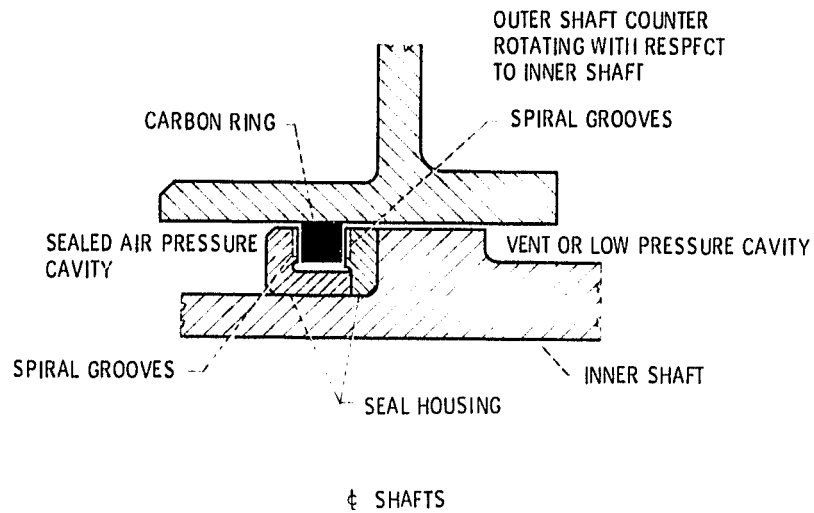


Figure 1. - Spiral groove inter-shaft ring seal.

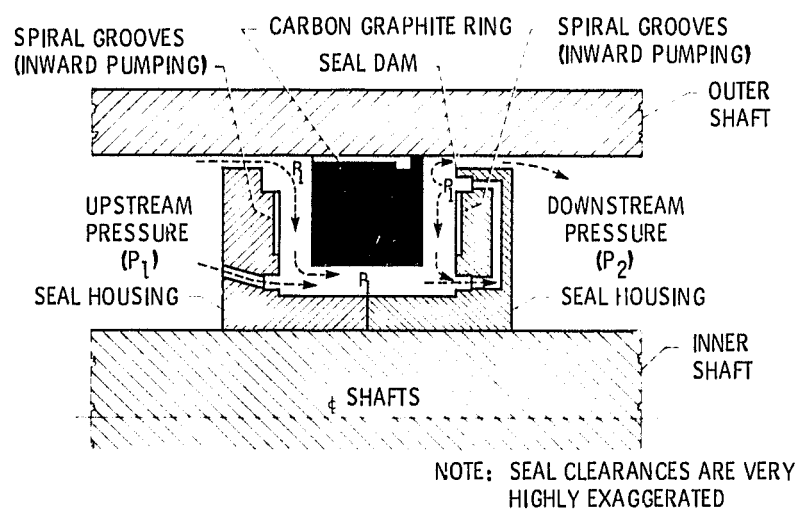


Figure 2. - Schematic of inter-shaft ring seal.

ORIGINAL PAGE IS
OF POOR QUALITY

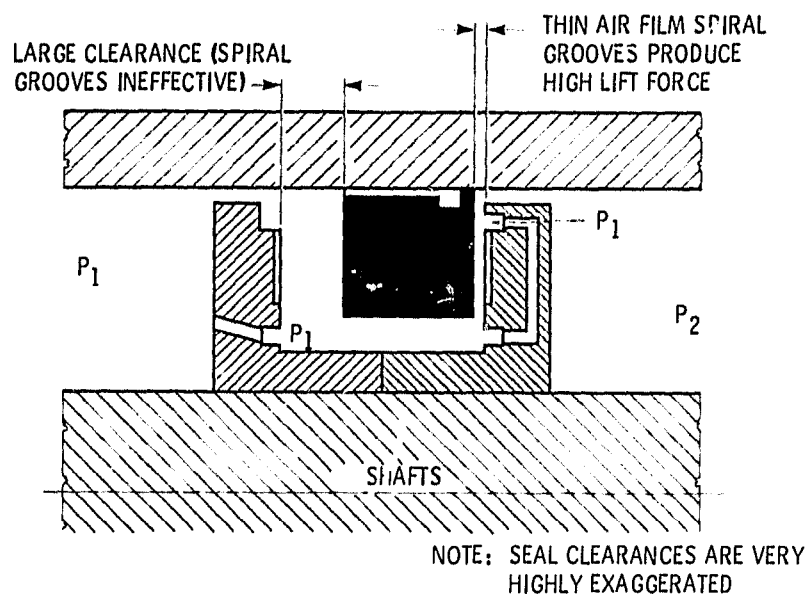


Figure 3. - Schematic showing seal ring displaced toward housing face.

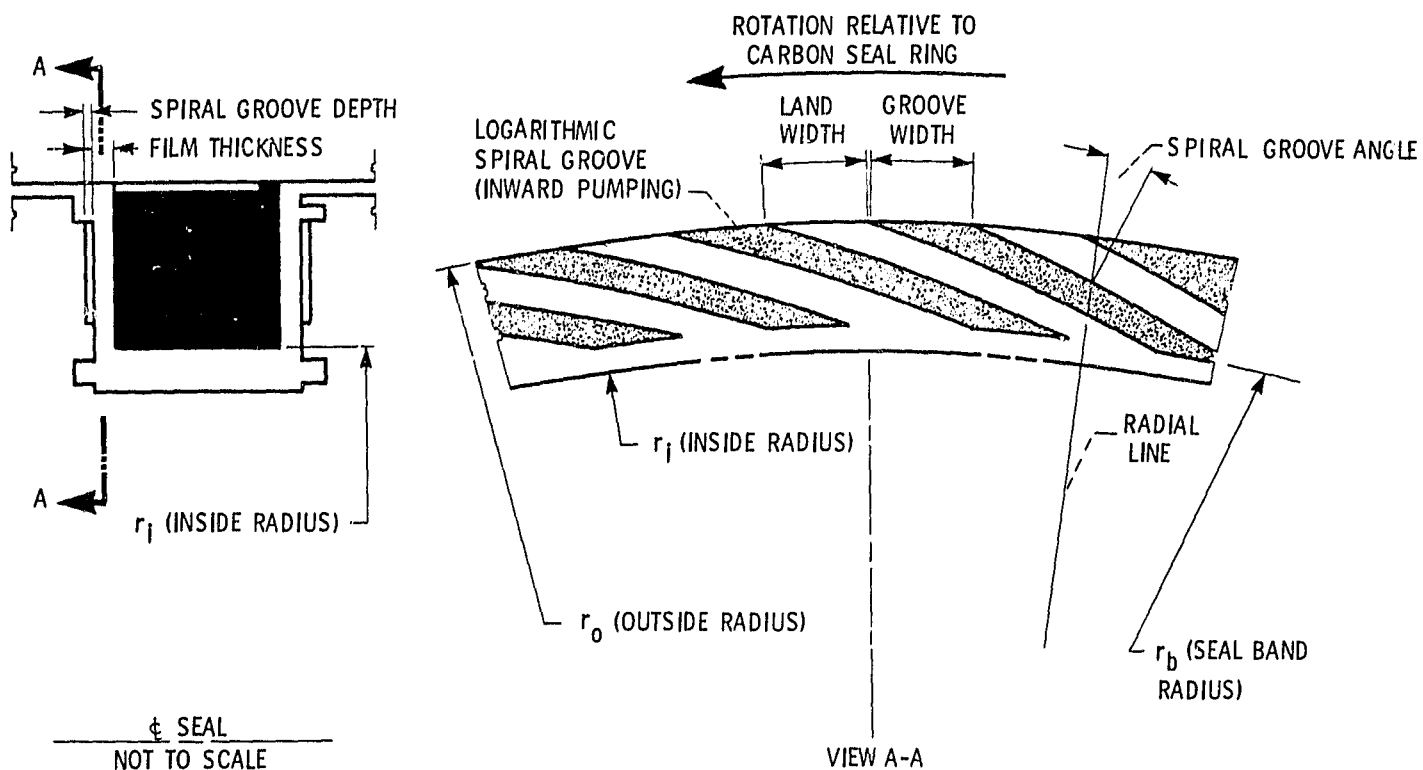


Figure 4. - Spiral groove ring seal geometry and nomenclature.

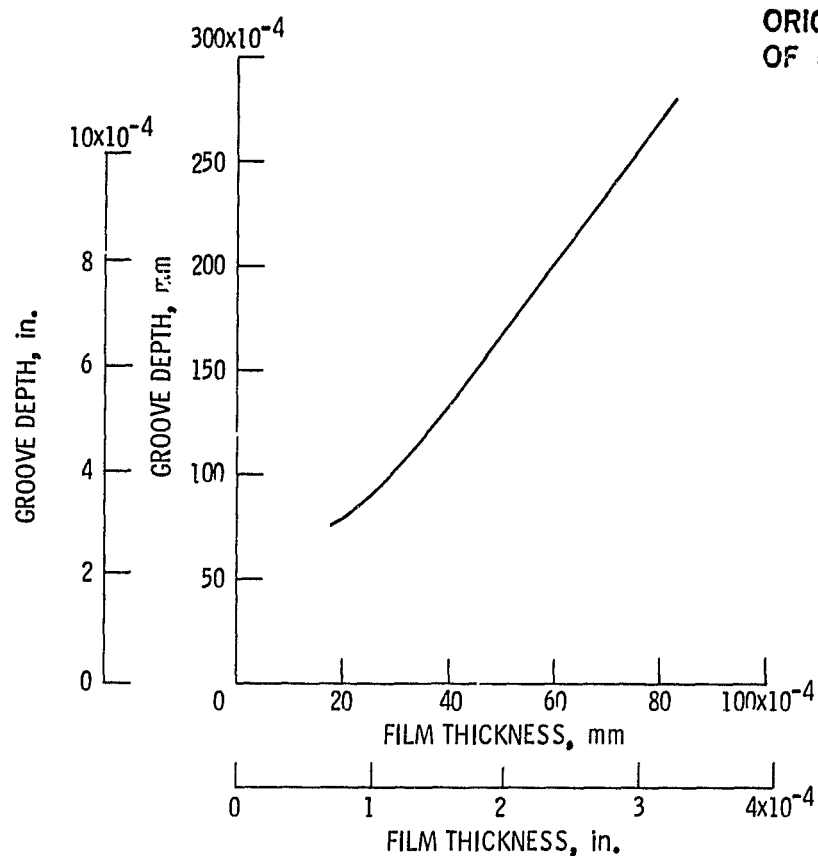


Figure 5. - Groove depth for maximum lift force as function of film thickness: spiral groove angle, 20° ; groove to land width ratio, 2.50; outside radius, 7.945 cm (3.128 in.); inside radius, 7.386 cm (2.908 in.); seal band radius, 7.488 cm (2.948 in.); engine operating condition 1.

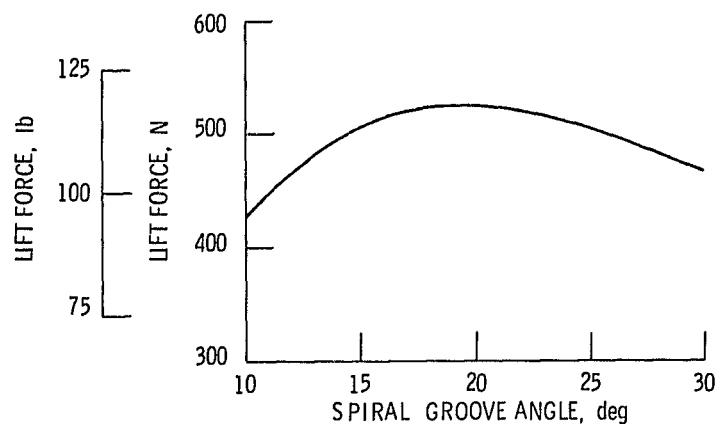


Figure 6. - Lift force as function of spiral groove angle: film thickness, 0.0051 mm (0.0002 in.); groove depth, 0.0178 mm (0.0007 in.); groove to land width ratio, 2.50; outside radius, 7.945 cm (3.128 in.); inside radius, 7.386 cm (2.908 in.); seal band radius, 7.488 cm (2.948 in.); engine operating condition 1.

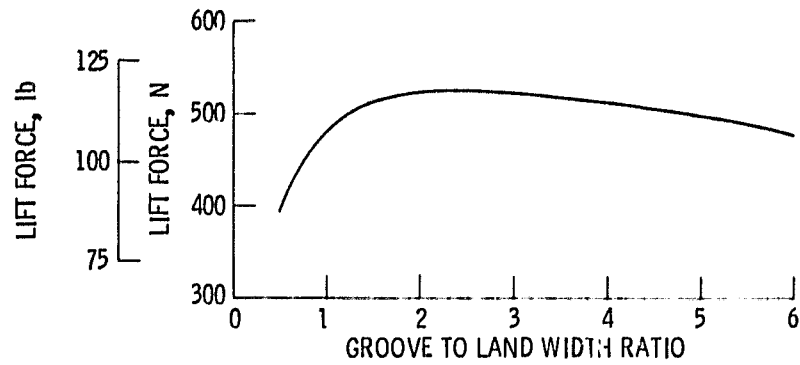


Figure 7. - Lift force as function of groove to land width ratio: film thickness, 0.0051 mm (0.0002 in.); spiral groove angle, 20° ; groove depth, 0.0178 mm (0.0007 in.); outside radius, 7.945 cm (3.128 in.); inside radius, 7.386 cm (2.908 in.); seal band radius, 7.488 cm (2.948 in.); engine operating condition 1.

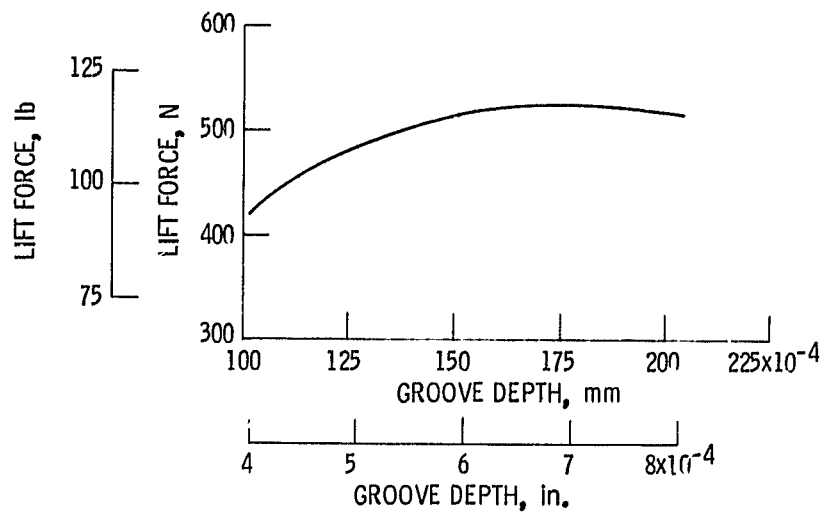


Figure 8. - Lift force as function of groove depth: film thickness 0.0051 mm (0.0002 in.); spiral groove angle, 20° ; groove to land width ratio, 2.50; outside radius, 7.945 cm (3.128 in.); inside radius, 7.386 cm (2.908 in.); seal band radius, 7.488 cm (2.948 in.); engine operating condition 1.

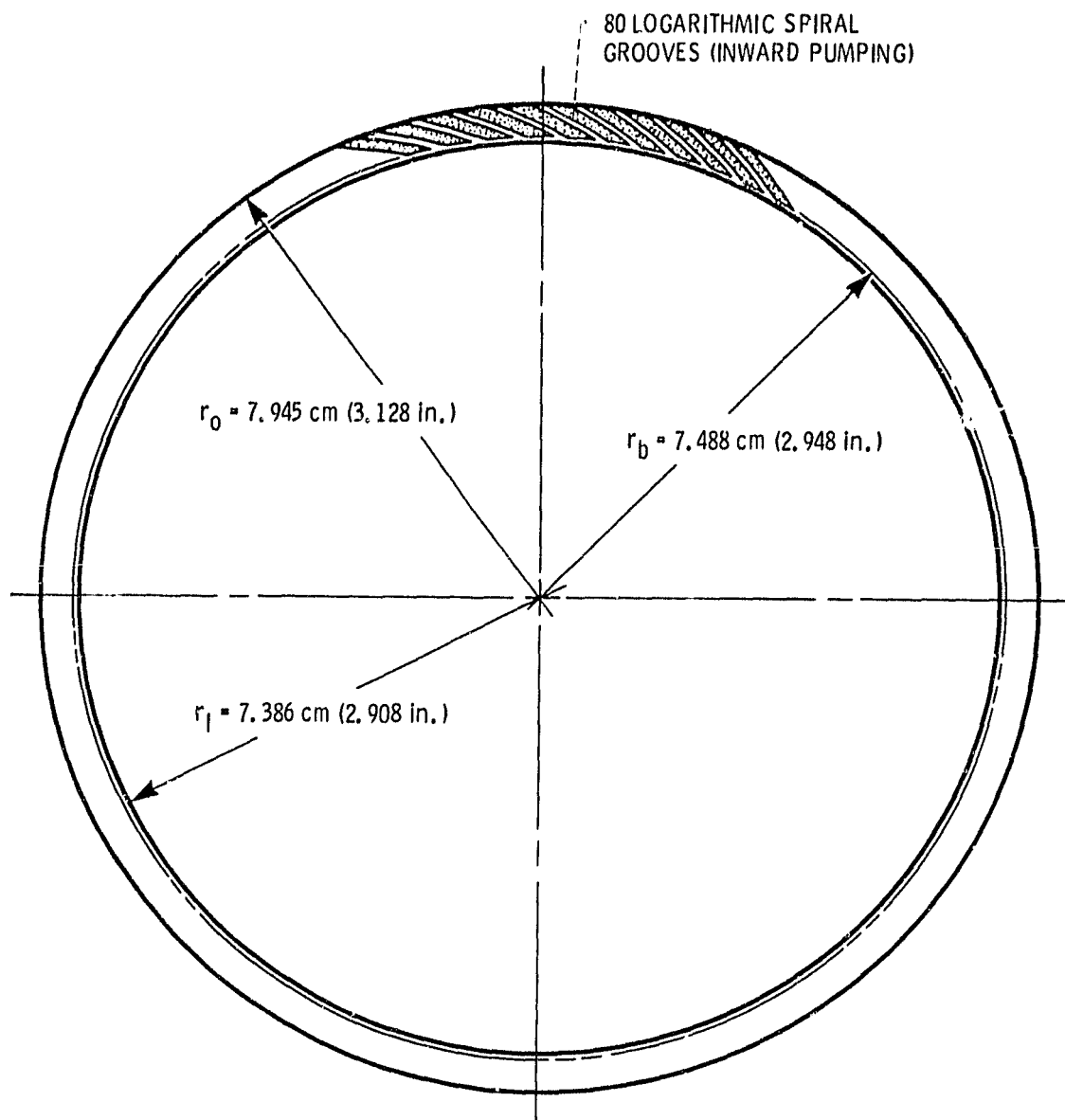


Figure 9. - Optimized logarithmic spiral grooves shown to scale. Spiral groove angle, 20° ; groove to land width ratio, 2.50.

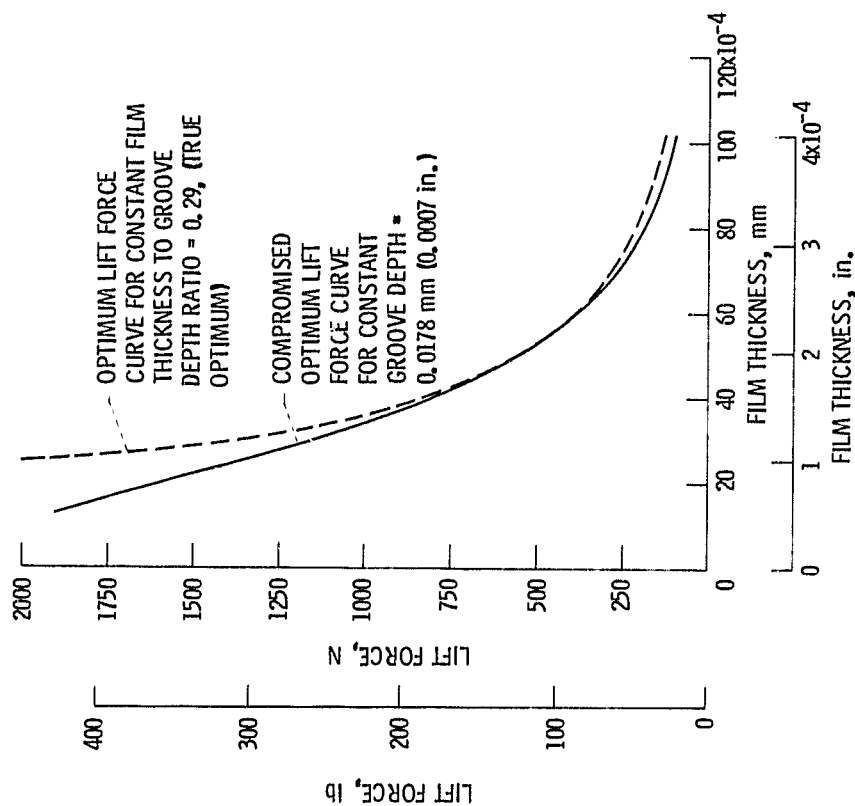


Figure 10. - Lift force as function of film thickness: spiral groove angle, 20° ; groove to land width ratio, 2.50; outside radius, 7.945 cm (3.128 in.); inside radius, 7.386 cm (2.908 in.); seal band radius, 7.488 cm (2.948 in.); engine operating condition 1.

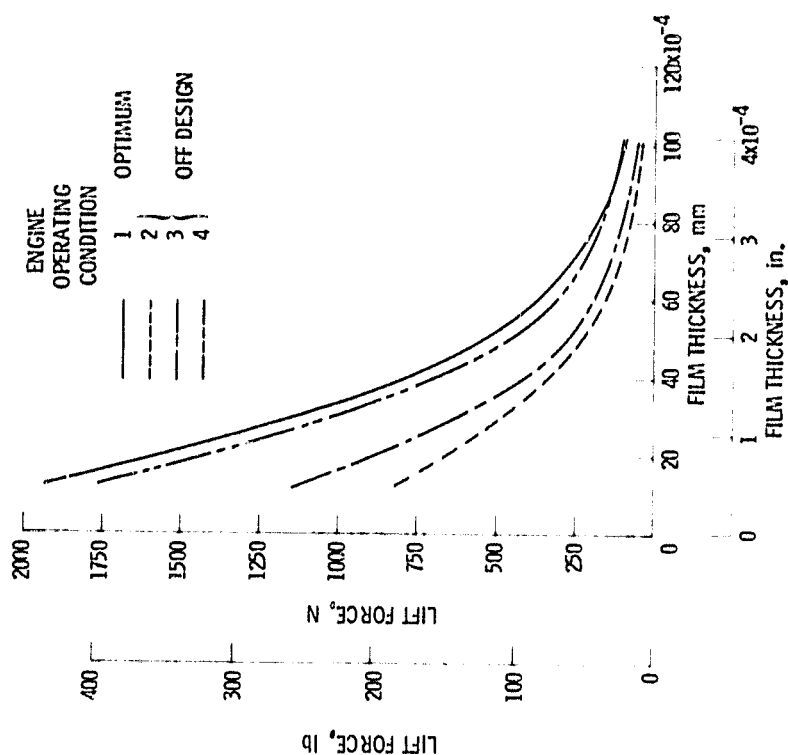


Figure 11. - Lift force as function of film thickness: spiral groove angle, 20° ; groove depth, 0.0178 mm (0.0007 in.); groove to land width ratio, 2.50; outside radius, 7.945 cm (3.128 in.); inside radius, 7.386 cm (2.908 in.); seal band radius, 7.488 cm (2.948 in.).